ISSN 2004-2965 Energy Proceedings, Vol. 18, 2021

International Conference on Applied Energy 2021
Nov. 29 - Dec. 2, 2021, in Bangkok, Thailand
Paper ID: 280

Proton exchange membranes doped with Prussian blue analogue for performance enhancement under low humidity conditions

Mengyuan Li, Xin Liu, Na Xie, Haotian Liu, Junfeng Zhang, Yan Yin*

State Key Laboratory of Engines, Tianjin University

ABSTRACT

In this study, Prussian blue analogue (PBA) with high content of lattice water is synthesized by a simple aqueous phase method and introduced into the sulfonated polysulfone (SPSf) polymer matrix, to prepare composite proton exchange membranes (PEMs) by solution casting method. The successful synthesis of PBA and the features of lattice water are comprehensively studied via X-ray diffraction (XRD), as well as several other characterization, reflecting considerable potential to promote Grotthuss type proton transport. In terms of membrane structure, XRD tests show that the PBA could be well dispersed in the SPSf matrix with the filler loading of 0-1.5 wt%. Mechanical strength, swelling ratio and water uptake were reduced in SPSf/PBA composite membranes with increased filler loading, within the appropriate range for PEM usage. The proton conductivity of SPSf/PBA composite membranes show evident improvements over pristine SPSf membrane, especially when relative humidity (RH) decreases. This result shows that the SPSf/PBA composite membranes are promising for use at low RH conditions, owing to the PBA filler containing abundant lattice water which helps facilitate Grotthuss type proton transport.

Keywords: Proton exchange membrane fuel cell, Composite membrane, Prussian blue analogue, Low relative humidity, Enhanced proton conductivity

1. INTRODUCTION

With high proton conductivity and chemical stability at low temperatures, Nafion® perfluorinated sulfonic acid membranes have been widely used in commercial proton exchange membrane fuel cell (PEMFC) stacks. However, Nafion® membranes lose water dramatically under the condition of high temperature and low relative humidity (RH), resulting in the decrease of proton conductivity [1]. For most PEMFC systems, water is provided externally and controlled by a water management subsystem [2]. However, it adds additional mass and size and causes the complexity of manufacture and assembling. Therefore, the water retention performance of proton exchange membrane (PEM) at higher temperature and lower RH becomes a critical problem with much research attention [3].

The general expression of Prussian blue analogue (PBA) is $M_3[M'(CN)_6]_2 \cdot xH_2O$, where M and M' are transition metals. It has a microporous frame structure similar to the zeolite, which usually contains a large amount of interstitial crystal water [4]. Due to the multi-void frame structure of NiFe-PBA, this kind of Prussian blue compound nanoparticles is expected to improve the water retention performance of PEMs. Under the condition of high temperature and low humidity, PEMs lose free water noticeably, so the proton conduction is mainly achieved through Grotthuss mechanism. When PBAs are introduced into proton exchange membranes, a large number of hydrogen bond networks between lattice water provide channels for the Grotthuss mechanism [5, 6]. Therefore, through the introduction of PBA, the proton exchange membrane can acquire well distributed water suitable for Grotthuss type transport even at low RH, and the high proton conductivity of PEMFC can be realized [7, 8].

In this study, NiFe-PBA is introduced into the sulfonated polysulfone (SPSf) polymer matrix to optimize the overall proton transport, thereby improving the membrane performance at low RH conditions.

2. EXPERIMENTAL

2.1 *Material and methods*

Sulfonated polysulfone (SPSf, Degree of Sulfonation =60%) was purchased from Shandong Jinlan Special

Selection and peer-review under responsibility of the scientific committee of the 13th Int. Conf. on Applied Energy (ICAE2021).

Polymer, China. Nickel sulfate ($NiSO_4$, 99%), potassium ferricyanide ($K_3Fe(CN)_6$, 99.5%) and phenolphthalein ($C_{20}H_{14}O_4$, 98%) were obtained from Aladdin, China. Sulfuric acid (H_2SO_4, 99%) were purchased from Tianjin Jiangtian chemical technology Co. Ltd. Dimethylformamide (DMF, 99.8%) was produced from Acros.

NiFe-PBA is synthesized using water thermal synthesis. $NiSO_4$ solution (40 mL 0.2 mol L^{-1}) was added to $K_3Fe(CN)_6$ solution (40 mL 0.1 mol L^{-1}) and stirred. After 6 h of the reaction, to remove the unreacted chemicals, the resulting precipitate was washed and centrifuged five times with a deionized aqueous solution. The precipitates were then dried at room temperature. NiFe-PBA was quantitatively dispersed and dissolved in DMF, and a uniformly stable mixed solution was obtained by ball mill ball grinding. In terms of membrane preparation, a fraction of PBA, was added at 0.5 wt%, 1 wt%, 1.5 wt% in the SPSF matrix to prepare a series of composite membranes. The membrane material was dissolved in 3.5 ml DMF and shaken well for 12 hours to obtain a uniform membrane solution. The membrane was prepared by evaporation in an oven at 80 °C for 12 hours. The prepared membranes were soaked in 1 M H_2SO_4 for 24 h, and washed with deionized water to remove the excess H_2SO_4 solution.

2.2 *Characterization*

NiFe-PBA was measured by X-ray diffraction (XRD) using a MiniFlex600 X-ray diffractometer (Rigaku, Japan) with a Cu Kα radiation generator. The Fourier transformed infrared tests (FTIR) of NiFe-PBA was recorded on NicoletiS10 system in the range of 4000–500 cm^{-1}.

The rectangular membranes samples were characterized by tensile test on a E1000 system tensile tester with the tensile speed was set as 2 mm min^{-1}.

Before measuring the swelling ratio (SR) and water uptake (WU) (%) of the membrane samples, they were placed in a vacuum drying oven at 80 °C for 24 hours to remove water. The dimensions and weight of the dry membranes are recorded as W_{wet} and L_{wet}. During the test, the membrane samples were immersed in deionized water at room temperature for 24 h. The dimensions and weight of the sample membranes after complete water absorption were recorded as W_{dry} and L_{dry}. The the SR and WU (%) of the sample membranes were calculated by the following formula:

$$\mathrm{WU} = \frac{W_{\mathrm{wet}} - W_{\mathrm{dry}}}{W_{\mathrm{dry}}} \times 100\% \quad (1)$$

$$\mathrm{SR} = \frac{L_{\mathrm{wet}} - L_{\mathrm{dry}}}{L_{\mathrm{dry}}} \times 100\% \quad (2)$$

The data results are obtained by averaging the tests repeated three times.

The IEC (mmol g^{-1}) was tested by acid-base titration. The dried membrane samples were immersed in a 15% mass fraction sodium chloride solution of 24 hours. This is done to fully exchange the protons with the Na^+ ions. The exchanged solutions were calibrated using standard concentrations of sodium hydroxide in response to phenolphthalein indicators. The IEC was calculated using the formula below:

$$\mathrm{IEC} = \frac{(V_{\mathrm{NaOH}} \times N_{\mathrm{NaOH}}) \times 1000}{W_{\mathrm{dry}}} \quad (3)$$

where V_{NaOH} is the consumed NaOH aqueous solution volume, the solution molar concentration of NaOH and W_{dry} is the mass of the membrane when drying.

Testing of the proton conductivity (σ, mS cm^{-1}) is usually calculated by the following formula:

$$\sigma = \frac{\mathrm{L}}{A \times R} \quad (4)$$

where L (cm) is the distance between the electrodes, A (cm^2) is the membrane surface area and R is the membrane resistance.

Equation (5) is introduced in the results of proton conductivity analysis.

$$\mathrm{IR}_{\sigma} = \frac{\sigma_{\mathrm{SPSf\text{-}}X} - \sigma_{\mathrm{SPSf}}}{\sigma_{\mathrm{SPSf}}} \times 100\% \quad (5)$$

Where IR_σ (%) is the relative increase rate of σ and *X* is representation of NiFe-PBA.

3. RESULTS AND DISCUSSION

3.1 *Synthesis results of NiFe-PBA*

Samples were qualitatively analyzed using X-ray diffraction. The structural components of the PBA material can be analyzed. As shown in Figure 1, the peak is corresponds to (200), (220), (400), and (420) crystals at 17.5°, 24.8°, 35.3°, and 39.6°, respectively. These peaks can be indexed to the surface-cubic structure (JCPDS No.46-0906), successful preparation of PBA, without other impurities was confirmed. Fig.1b shows the Fourier-transform infrared spectra of PBA, PBA with a strong absorption peak at 2184 cm^{-1}, which is attributed to the characteristic vibration of -C≡N-. The absorption peak at ~3378 cm^{-1} is associated with the PBA internal lattice water.

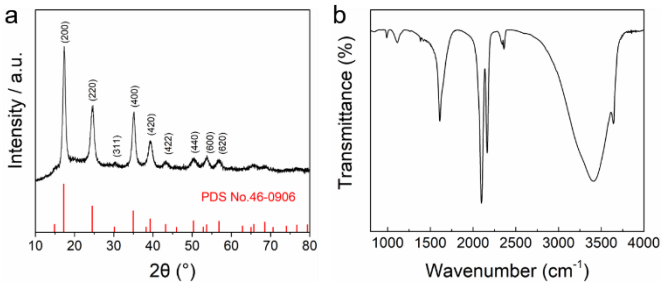

Fig.1 (a) XRD pattern and (b) FTIR spectra of PBA

The physical properties of PBA were further characterized by thermogravimetric analysis (TGA) and differential scanning calorimetry (DSC). As shown in Fig. 2a, the previous mass loss of 150 °C can be attributed to the removal of adsorbed water and gap water in the structure, with the sample PBA having a water content of 1 wt%., respectively. From 150 °C to 220 °C, the weight was rapidly eliminated due to the loss of the -C≡N- group. From 220 °C to 800 °C, a heat absorption reaction was involved. It may be involved in multiple complex reactions such as breakdown of the skeleton, metal carbide formation and release of gas.

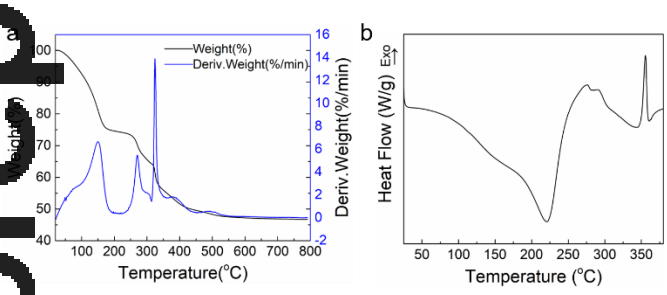

Fig.2 (a) TGA pattern and (b) DSC spectra of PBA

3.2 Synthesis results of SPSf/PBA composite membranes

Fig.3. presents the XRD patterns of SPSf/PBA composite membranes. The pure SPSf membrane has an amorphous peak at 22.66°, corresponding to the arrangement of the polymer backbone in the hydrophobic phase. The unstereotyped peaks of the composite membrane shift left as the PBA mass fraction increases. It suggests that the increased molecular chain spacing of the polymer is related to the introduction of PBA nanofillers. This implies that the PBA in the hydrophobic polymer backbone phase is consistent with the properties of the PBA hydrophobic framework structure. There are no significant PBA characteristic peaks in the XRD curve of the composite membrane of SPSf/PBA as compared to the XRD plot of PBA. It suggests that PBA did not agglomerate in the membrane, resulting a homogeneous composite membrane.

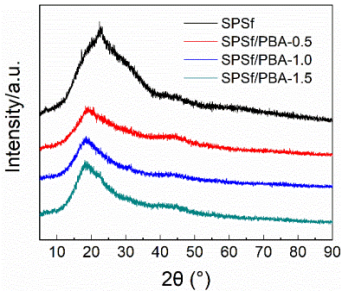

Fig.3 The XRD patterns of different composite membranes

3.3 Mechanical property

Table 2 shows the mechanical property data of SPSf and SPSf/PBA composite membranes. Under the same test conditions, the mechanical tensile strength and Young's modulus of SPSf/PBA-0.5 and SPSf/PBA-1.0 composite membrane are not different from that of SPSf. However, compared with the original SPSf, the mechanical tensile strength and young's modulus of SPSf/PBA-1.5 composite film are reduced by 9 MPa and 231MPa. This may be due to the introduction of more PBA fillers in SPSf/PBA-1.5 composite membrane, which makes the internal connection of the membrane not close enough. According to the results of elongation at break, the addition of PBA filler has a slightly weakened effect on the brittleness of the membrane.

Tab.1 Mechanical properties of SPSf and SPSf/PBA

Membrane	Tensile strength [MPa]	Young's modulus [MPa]	Elongation at break [%]
SPSf	41.75	810	10.2
SPSf/PBA-0.5 (0.5wt%)	40.58	785	7.3
SPSf/PBA-1 (1.0wt%)	37.97	725	8.2
SPSf/PBA-1.5 (1.5wt%)	32.77	579	6.4

3.4 WU, SR and IEC

Table 2 summarizes the WU, SR, IEC, σ and TS. of the SPSf and SPSf/PBA composite membranes. It is well known that the physicochemical properties of PEM directly affect the energy efficiency and service life of fuel cell systems. WU and IEC have a large effect on the membrane conductance conductivity. In general, higher WU and IEC values would increase the proton

conductivity of the PEM. Clearly, the WU and IEC of the SPSf/PBA complex membrane decreased with the PBA nanofiller content compared to the original SPSf membrane. This is due to the addition of inorganic nanoparticles leading to the decrease of the free space in the membrane. The decrease in the complex membrane IEC is due to the low IEC of the PBA nanoparticles themselves. When the nanofillers are added to the SPSf substrate, the IEC of the mixture will decrease. Second, with the increased intramembrane content of PBA nanoparticles, PBA nanoparticles will occupy groups and sites available for ion exchange in the original SPSf membrane, resulting in an increase in effective IEC loss. However, the proton conductivity of the SPSF/PBA composite membrane is improved when compared to the original SPSf membrane.

This is attributed to the octahedral cube structure of PBA containing lattice water and the continuous hydrogen bonding network, providing a Grotthuss mechanism for proton conduction. Thus, the σ value of the PBA complex membranes is increased. Therefore, σ can be improved by adding PBA nanocrystalline fillers to the SPSf membrane. Furthermore, their tensile strength does not differ much. Therefore, it is shown that the introduced PBA nanoparticle packing has no evident negative effect on the mechanical properties of the SPSf membrane matrix.

Tab.2 Properties of SPSf and SPSf/PBA

Membrane	σ^a [mS cm^{-1}]	SR [%]	WU [%]	IEC [mmol g^{-1}]
SPSf	73.29	25.06	54.16	1.97
SPSf/PBA-0.5 (0.5wt%)	80.85	24.36	56.08	1.96
SPSf/PBA-1 (1.0wt%)	98.56	20.48	52.12	1.77
SPSf/PBA-1.5 (1.5wt%)	108.12	19.78	50.73	1.76

a: Measurement at room temperature at 100% RH

3.5 Proton conductivity

The σ of SPSF/PBA composite membranes with different PBA nanoparticle content is shown in Fig. 4a. It shows all membranes increase with increasing RH at room temperature of 25 °C and σ reaches its maximum at 100% RH. The σ of SPSf/PBA composite membranes membrane is higher than that of the original SPSf. The SPSf/PBA-1.5 composite membrane showed the best performance of σ compared with the other membranes at low relative humidity (30% RH - 60% RH), especially. Compared with pure SPSf, although the water content of SPSf/PBA composite membranes decrease, the proton conductivity increases. Fig. 6b shows that the σ of SPSf/PBA-1.5 composite membrane is increased by 140% compared with the original SPSf membrane. The IR_σ of SPSf/PBA-1 and SPSf/PBA-1.5 composite membranes are excellent at low humidity. It indicates that PBA lattice water plays a dominant role in the optimization of proton conduction mode. The effect of free water content in composite film is weak.

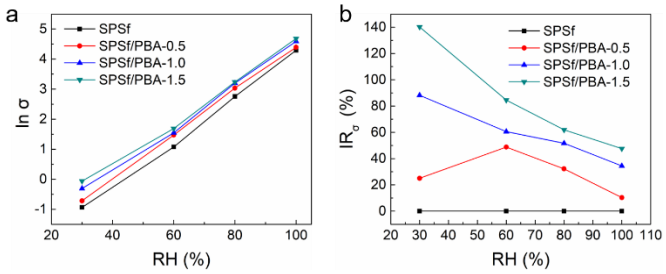

Fig.4 (a) Line diagram of lnσ of SPSf and SPSf/PBA composite membranes. (b) Line diagram of IR_σ of SPSf and SPSf/PBA composite membranes.

PBA is an open frame structure with abundant lattice hydrogen bond network. The above results fully verified the introduction of PBA nanoparticles into SPSf matrix, thus introducing a large number of water molecules with continuous hydrogen bond network into the original SPSf membrane. This contributes to proton conduction in Grotthuss and improves the original SPSf membrane σ.

4. CONCLUSION

The composite membrane with a high proportion of lattice water molecule is prepared by solution casting, and PBA is introduced into the SPSF polymer matrix. The PBA packing was successfully synthesized by the XRD and FTIR tests, and a proportion of nonfreezing water and better thermal stability within the PBA packing was characterized by the TGA and DSC tests. In terms of membrane structure, XRD tests show that the PBA packing is better dispersed in the polymer matrix (SPSf). When controlling the packing amount to 1wt%, the tensile strength of the film is not weakened. Compared with the original SPSf membrane, the SPSf/PBA composite membrane has a reduced swelling rate and

water absorption rate, and the proton conductivity has been improved, especially in the low relative humidity conditions. This shows that the SPSf/PBA complex membrane has excellent anti-dissolution resistance and excellent proton conductivity, which is expected to be widely used in high temperature and low RH proton exchange membrane fuel cells.

ACKNOWLEDGEMENT

This research is supported by National Natural Science Foundation of China (22005214 and 21875161).

REFERENCE

[1] Zhang H, Shen PK. Recent Development of Polymer Electrolyte Membranes for Fuel Cells. Chem Rev 2012; 112: 2780-832.

[2] Liu ZC, Shen J, Pei HC, Tu ZK, Wang J, Wan ZM, Liu W. Effect of humidified water vapor on heat balance management in a proton exchange membrane fuel cell stack. Int J Energy Res 2015; 39: 504-15.

[3] Park CH, Lee CH, Guiver MD, Lee YM. Sulfonated hydrocarbon membranes for medium-temperature and low-humidity proton exchange membrane fuel cells (PEMFCs). Prog Polym Sci 2011; 36: 1443-98.

[4] Ma F, Li Q, Wang TY, Zhang HG, Wu G. Energy storage materials derived from Prussian blue analogues. Sci Bull 2017; 62: 358-68.

[5] Wu X, Hong JJ, Shin W, Ma L, Liu T, Bi X, Yuan Y, Qi Y, Surta TW, Huang W, Neuefeind J, Wu T, Greaney PA, Lu J, Ji X. Diffusion-free Grotthuss topochemistry for high-rate and long-life proton batteries. Nat Energy 2019, 4(2): 123-30.

[6] Lee J-H, Ali G, Kim DH, Chung KY. Metal-Organic Framework Cathodes Based on a Vanadium Hexacyanoferrate Prussian Blue Analogue for High-Performance Aqueous Rechargeable Batteries. Adv Energy Mater 2017, 7(2): 1601491.

[7] Vilciauskas L, Tuckerman ME, Bester G, Paddison SJ, Kreuer KD. The mechanism of proton conduction in phosphoric acid. Nat Chem 2012; 4: 461-6.

[8] Lim DW, Kitagawa H. Proton Transport in Metal-Organic Frameworks. Chem Rev 2020, 120(16): 8416-67.